Journal of Applied Research and Technology

www.jart.icat.unam.mx

Journal of Applied Research and Technology 23 (2025) 513-524

Original

Toward multi relay selection aided two-way multi-users cooperative GSPIM-DCSK communication system

B. Nazar*[1] • F. S. Hasan[1]

[1]*Electrical Engineering. Department, Mustansiriyah University, College of Engineering., Iraq, Baghdad*

Received 10 27 2024; accepted 11 25 2024
Available 10 31 2025

Abstract: To improve the error quality of a single-relay two-way half-duplex cooperative communication system based on a Joint Grouping Subcarrier and Permutation Index Modulations DCSK (GSPIM-DCSK), a novel multi-relay two-way multi-user half-duplex cooperative communication system is offered in this work. The GSPIM-DCSK scheme serves as the foundation for this system's architecture. In this system, many relays are established, but during the relaying phase, only one relay is used to transmit network-coded data to the consumers. Every relay node in this network is assumed to be using the protocol method called Decode and Forward (DF). To determine which relay should be chosen, the max-sum (M_S), max-min (M_M), and max-product (M_P) relay-selection methodologies are employed. Particularly, these requirements are used at the relay's reception to produce two judgment numbers, which are subsequently subjected to further processing via procedures such as sum, product, or min. The parameters of all relays are then compared to see which one is more reliable for relaying after this process. The performance of the novel system is evaluated by acquiring and applying the simulation findings at multipath Rayleigh fading channels. Furthermore, a comparative analysis is conducted between the cooperative system-based DCSK and GSPIM-DCSK that utilizes a single relay and a novel cooperative-based GSPIM-DCSK system that utilizes multiple relays. The average bit error rate (BER) performance is included in this. Moreover, an examination shows how the suggested cooperative system raises the effectiveness of traditional cooperative systems.

Keywords: Multi-relay, relay selection, two-way, multi-user, cooperative two-relay, GSPIM-DCSK.

*Corresponding author.
E-mail address: besma.nazar@uomustansiriyah.edu.iq (B. Nazar).
Peer Review under the responsibility of Universidad Nacional Autónoma de México.

1. Introduction

Radio communications use chaotic system-instituted modulation techniques because of their minimal objection risk, flexibility, and signal fading. These systems are capable of producing an infinite number of chaotic sequences by adjusting the beginning circumstances, supporting many users, and utilizing simple circuit designs for both modulation and demodulation (Aboltins et al., 2023; Bai et al., 2019; Que et al., 2021; Rasool, M., & Belhaouari, , 2023). Because non-coherent chaotic modulation is simpler and does not require complicated synchronization or channel state estimation, it is a more attractive option than coherent modulation. Differential chaos shift keying (DCSK) is an important system, however it is inefficient since it needs delay lines for the demodulation process and uses half of the symbol time and energy to broadcast a reference chaotic sequence. Through the removal of delay lines and the achievement of legitimate data transfers at faster speeds, researchers are increasing efficiency and practicality (Chen et al., 2021; Kaddoum, 2016). By expanding DCSK in parallel, the Multi-Carrier DCSK (MC-DCSK) improves both spectrum and energy efficiency (Kaddoum et al., 2013). To improve the data bit rate and handle delay line problems, the Orthogonal Frequency Division Multiplexing DCSK (OFDM-DCSK) system is introduced in (Li et al., 2015). Multiple-antenna systems and other diversity devices are frequently used in wireless networks to reduce signal fading, but their deployment can be expensive and challenging. By sharing antennae, users can connect thanks to cooperative diversity (Xu et al., 2010). Research has suggested collaborative strategies that employ a variety of modulation techniques to accomplish performance objectives. The Physical Layer Network Coding (PNC) scheme between two nodes is presented in (Kaddoum & El-Hajjar,, 2015). It employs the same spreading sequence and bandwidth, but the influence of multipath fading channels causes performance degradation. To solve this problem, two alternative networking coding systems are presented, which enable every client to transmit their data at an independent frequency or time. To increase performance, the investigation in (Cai et al., 2017) adds equal gain aggregating methods and uses the DF protocol for data decoding and XOR in a cooperative two-relay, two-way DCSK modulation system. The max-sum (M_S), max-min (M_M), and max-product (M_P) methods were also included as options for selection for improving performance. Its proposal for three-way relay network coding systems, based on DCSK, proposes two physical layer network coding (PLNC) systems for transmission between three-users (Hasan, 202). First, data from each user was sent to the relay using three different time slots; second, a multiple-user approach using QPSK modulation in the second phase and Gram Schmidt in the first, boosts system throughput. In contrast to conventional SR-DCSK and DCSK cooperative systems, the CIM-SR-DCSK-CC system, which was proposed in (Fang et al., 2022), is a high-throughput cooperative system with code index modulation (CIM) and short reference (SR), increasing system throughput. A novel two-way half-duplex cooperative network constructed around a Joint Grouping Subcarrier Permutation Index Modulation DCSK (GSPIM-DCSK) is presented in ((Nazar & Hasan, 2023b; Nazar & Hasan, 2024a; Nazar & Hasan, 2024b) where two parties wish to interact with each other over a single relay to boost energy consumption, data capacity, and BER quality. To enhance error performance in a two-way half-duplex cooperative communication system based on a GSPIM-DCSK modulation scheme, we suggest in this study replacing a single relay in a multi-user cooperative communication system with a multi-relay. Instead of using a single relay to transmit network-coded data, the system employs many relays. The system chooses the relay by utilizing relay selection algorithms, from reference (Cai et al., 2017). Our study is built upon the GSPIM DCSK method first presented in reference (Nazar et al., 2023a). Below is a summary of the contributions of our research:

- A cooperative system with a multi-relay-based GSPIM-DCSK modulation scheme is presented in this paper. This network allows multi-users to communicate with each other via relays in a two-way half-duplex mechanism with decode and forward protocol (DF) in each relay. To eliminate the interference between users, each user transmits their information data to the relay at a different time. Not all relays are used for transition just one is chosen which makes the overall performance of the network better. The criteria proposed in (Cai et al., 2017) are used for choosing the relay that provides reliable communication between users in the network. Based on this criterion, three relay methods for selection are developed: the max-sum (M_S), max-min (M_M), and max-product (M_P). Particularly, these standards are used at the relay's reception to produce two deciding values, which are subsequently subjected to further processing via procedures such as sum, product, or min. The parameters of the two relays are compared to see which is more dependable for transmission after this process.

- The performance of the novel system is evaluated by acquiring and applying the simulation findings at multipath Rayleigh fading channels. Furthermore, a comparative analysis is conducted between the cooperative system-based DCSK and GSPIM-DCSK that utilizes a single relay and a novel cooperative-based GSPIM-DCSK system that utilizes multiple relays. The average bit error rate (BER) performance is included in this.

The paper is structured as follows: An overview of the GSPIM-DCSK technology may be found in the next section. The novel multi-relay, two-way, multi-user GSPIM-DCSK cooperative network with relay-selection algorithms is described in Section 3. Section 4 presents the system performance regarding link spectral efficiency, throughput, and average BER. The findings of the research are given in the last part.

2. An Overview of GSPIM-DCSK Scheme

To broadcast a chaotic reference signal out of a total of ($2^{\mathfrak{p}}$ +1) ones, the GSPIM-DCSK transmission technique employs a single subcarrier at frequency f_0 . Grouping subcarrier index modulation is another technique used by this modulation system to accomplish its objectives. The sender side divides up each of the G sets of input bits, which include modulated, carrier, and permutation bits. Each group's active and inactive subcarriers are identified among $2^{\mathfrak{p}1}$ subcarriers by the carrier index bits. This gives rise to two distinct GSPIM-DCSKI and GSPIM-DCSKII schemes, each with a unique mechanism for selecting active and inactive subcarriers. A permuted representation of a reference sequence is generated by a permutation function that is determined by the permutation index bits. After that, a modulated data bit is distributed using this permuted form and sent via efficient subcarriers. A chaotic function is used to construct the reference signal, which has a length of β chips. It is then passed to the permutation unit, which generates $2^{\mathfrak{p}2}$ quasi-orthogonal permuted replicas of the original signal (Lau et al., 2003). In the GSPIM-DCSKI model, there are $(\mathfrak{p}1+\mathfrak{p}2+1)$ bits in each group. Therefore, a total of $G(\mathfrak{p}1+\mathfrak{p}2+1)$ bits are sent at each $\mathfrak{m}^{th}$ symbol time. Each group has a single modulated and carried bit, designated by $\mathfrak{p}1$ and $\mathfrak{p}2$, respectively, for the carrier index and permutation index bits. The conveyed data bits for the $\mathfrak{g}^{th}$ group and for the $\mathfrak{m}^{th}$ symbol time are, $\mathcal{S}_{\mathfrak{m}}^{\mathfrak{g}}:\{\mathfrak{a}_{\mathfrak{m},(\mathfrak{g}-1)\mathfrak{p}_t+1},\dots,\mathfrak{a}_{\mathfrak{m},(\mathfrak{g}-1)\mathfrak{p}_t+\mathfrak{p}_t}\}$, $\mathfrak{g}$ =1,...., G For each $\mathfrak{g}^{th}$ group, the carrier bits $(\mathfrak{a}_{\mathfrak{m},(\mathfrak{g}-1)\mathfrak{p}_t+1},\dots,\mathfrak{a}_{\mathfrak{m},(\mathfrak{g}-1)\mathfrak{p}_t+\mathfrak{p}1})$ are translated to a character $e_{\mathfrak{m}}^{\mathfrak{g}}\in[1, 2^{\mathfrak{p}1}]$. This character designates one of the 2p1carriers in that band as an effective carrier. The permuted form of the reference signal is obtained by mapping the permutation bits $(\mathfrak{a}_{\mathfrak{m},(\mathfrak{g}-1)\mathfrak{p}_t+\mathfrak{p}1+1},\dots,\mathfrak{a}_{\mathfrak{m},(\mathfrak{g}-1)\mathfrak{p}_t+\mathfrak{p}1+\mathfrak{p}2})$ to the symbol $pr_{\mathfrak{m}}^{\mathfrak{g}}\in[1, 2^{\mathfrak{p}2}]$, which selects one operator from the set of $2^{\mathfrak{p}2}$ permutation operators, $\mathcal{P}_{\mathfrak{r}}=[\mathcal{P}_{\mathfrak{r}1},\mathcal{P}_{\mathfrak{r}2},\dots,\mathcal{P}_{\mathfrak{r}\mathfrak{u}},\mathcal{P}_{\mathfrak{r}2^{\mathfrak{p}2}}]$, $\mathfrak{u}$ =1,..., $2^{\mathfrak{p}2}$. The last data bit in $\mathcal{S}_{\mathfrak{m}}^{\mathfrak{g}}$, $(\mathfrak{a}_{\mathfrak{m},(\mathfrak{g}-1)\mathfrak{p}_t+\mathfrak{p}_t})$, is modulated and converted to $\mathfrak{b}_{\mathfrak{m}}^{\mathfrak{g}}=(1,-1)$ via a polarity conversion. This modulated bit is then separated by the permuted form of the chaotic reference pulse chosen by the $\mathfrak{p}2$ bits. The presently picked carrier in each group then sends the modulated bit. For every group, the sequence $\mathfrak{r}$ =1,..,$2^{\mathfrak{p}1}$, $\mathfrak{g}$ =1,.., G is produced. If the $\mathfrak{r}^{th}$ subcarrier is alive, $d_{\mathfrak{m},\mathfrak{r}}^{\mathfrak{g}}$ equals to $\mathfrak{b}_{\mathfrak{m}}^{\mathfrak{g}}$; if not, it equals zero. Figure 1 shows the block layout of the GSPIM-DCSKI transmitter architecture. The system of chaos used to create the chaotic reference wave with β chips is the logistic map $x_{\mathfrak{m},k+1}=1-2x_{\mathfrak{m},k}^2$. The pulse shaping block's resultant signal is as follows:

$$x_{\mathfrak{m}}(t)=\sum_{k=1}^{\beta}x_{\mathfrak{m},k}\,\mathfrak{c}(t-kT_{\mathfrak{c}}) \tag{1}$$

where $T_{\mathfrak{c}}$ is the chip time and $\mathfrak{c}(t)$ is the square-root cosine filter. By multiplying the data-bearing pulse in each block of the GSPIM-DCSKI structure by the coefficients weight, $d_{\mathfrak{m},\mathfrak{r}}^{\mathfrak{g}}$, it may be modulated on the subcarriers with matching frequencies and combined to form the transmitted signal for the $\mathfrak{m}^{th}$ GSPIM-DCSKI symbol's period. This may be said in the following way:

$$\mathcal{S}_{\mathbb{T}}(t)=\sum_{\mathfrak{g}=1}^{G}\sum_{\mathfrak{r}=1}^{2^{\mathfrak{p}1}}d_{\mathfrak{m},\mathfrak{r}}^{\mathfrak{g}}\,cos\big(2\pi f_{(\mathfrak{g}-1)2^{\mathfrak{p}1}+\mathfrak{r}}t+\varphi_{(\mathfrak{g}-1)2^{\mathfrak{p}1}+\mathfrak{r}}\big)+x_{\mathfrak{m}}(t)cos(2\pi f_0 t+\varphi_0) \tag{2}$$

where the angle of phase $\varphi_{(\mathfrak{g}-1)2^{\mathfrak{p}1}+\mathfrak{r}}$ and carrier frequency $f_{(\mathfrak{g}-1)2^{\mathfrak{p}1}+\mathfrak{r}}$for the $\mathfrak{r}^{th}$ carrier in the $\mathfrak{g}^{th}$ block are supplied, respectively. The signal received among the $\mathbb{J}$ distinct Rayleigh distribution routes in the receiving section, each with coefficients $\lambda_{\mathfrak{j}}$ and a time delay $\tau_{\mathfrak{j}}$ (Cheng et al., 2016), (Hasan, 2021), is represented as follows:

$$\mathbb{y}(t)=\sum_{\mathfrak{j}=1}^{\mathbb{J}}\lambda_{\mathfrak{j}}\delta(t-\tau_{\mathfrak{j}})\otimes\mathcal{S}_{\mathbb{T}}(t)+\zeta(t) \tag{3}$$

The zero mean wide-band AWGN wave with $\mathbb{N}_o/2$ power density (PSD) is represented by ζ(t), and the convolution operator is represented by ⊗. The received GSPIM-DCSKI technique's block arrangement is shown in Figure 2. In this setup, the processor multiplies the sinusoidal frequencies ($2^{\mathfrak{p}}$ +1) that occur concurrently with the entering signal, $\mathbb{y}(t)$. Matching filters are employed to filter and sample the resulting ($2^{\mathfrak{p}}$ +1) strings at regular intervals of $kT_{\mathfrak{c}}$. After that, the recovered reference chaotic wave is permuted using a permutation device into $2^{\mathfrak{p}2}$ variations, which are then recorded in an $\boldsymbol{\mathcal{A}}_{2^{\mathfrak{p}2}\times\beta}$ matrix. The $\mathfrak{g}^{th}$ $\boldsymbol{\mathcal{B}}^{\mathfrak{g}}_{2^{\mathfrak{p}1}\times\beta}$ matrix contains the $2^{\mathfrak{p}1}$ data strings for each block. $\mathcal{Z}^{\mathfrak{g}}_{\mathfrak{m}}, \mathfrak{g} = 1,.., G$, the $\mathfrak{g}^{th}$ correlation matrices, are ultimately determined to be:

$$\boldsymbol{\mathcal{Z}}^{\mathfrak{g}}_{\mathfrak{m}} = \boldsymbol{\mathcal{A}} \times (\boldsymbol{\mathcal{B}}^{\mathfrak{g}})^T = \begin{bmatrix} \mathcal{Z}^{\mathfrak{g}}_{\mathfrak{m},(1,1)} & \cdots & \mathcal{Z}^{\mathfrak{g}}_{\mathfrak{m},(1,2^{\mathfrak{p}1})} \\ \vdots & \cdots & \vdots \\ \mathcal{Z}^{\mathfrak{g}}_{\mathfrak{m},(2^{\mathfrak{p}2},1)} & \cdots & \mathcal{Z}^{\mathfrak{g}}_{\mathfrak{m},(2^{\mathfrak{p}2},2^{\mathfrak{p}1})} \end{bmatrix}^T, \mathfrak{g} = 1,.., G \tag{4}$$

To get the recognized effective carrier, $\hat{e}^{\mathfrak{g}}_{\mathfrak{m}}$, and permutation, $\widehat{\mathfrak{pr}}^{\mathfrak{g}}_{\mathfrak{m}}$, indexes, the largest magnitude value $\mathcal{Z}^{\mathfrak{g}}_{\mathfrak{m},(\mathfrak{w},\mathfrak{r})}$, $\mathfrak{w}$ =1,…, $2^{\mathfrak{p}2}$, $\mathfrak{r}$ =1,.., $2^{\mathfrak{p}1}$ is obtained in the $\mathfrak{g}^{th}$ block. This value may be expressed as follows:

$$(\widehat{\mathfrak{pr}}^{\mathfrak{g}}_{\mathfrak{m}}, \hat{e}^{\mathfrak{g}}_{\mathfrak{m}}) = \arg \max_{\mathfrak{w}=1,..,2^{\mathfrak{p}2},\mathfrak{r}=1,..,2^{\mathfrak{p}1}} \left(\left|\mathcal{Z}^{\mathfrak{g}}_{\mathfrak{m},(\mathfrak{w},\mathfrak{r})}\right|\right) \tag{5}$$

The binary creation of such indices is accomplished by utilizing opposite mapping to transform the symbol shape into binary code. Take $\left[\hat{\mathfrak{a}}_{\mathfrak{m},(\mathfrak{g}-1)\mathfrak{p}t+2}, \dots, \hat{\mathfrak{a}}_{\mathfrak{m},(\mathfrak{g}-1)\mathfrak{p}t+\mathfrak{p}1}\right]$as an example. $(\boldsymbol{e}^{\mathfrak{g}}_{\mathfrak{m}})$, = Opposite Mapping, where $\mathfrak{g} = 1,.., G$. Finally, the modulated bit found in the $\mathfrak{g}^{th}$ sub-block is obtained using the following formulation:

$$\hat{\mathfrak{a}}_{\mathfrak{m},(\mathfrak{g}-1)\mathfrak{p}_t+1} = \begin{cases} 0 & if\ sign\left(\mathcal{Z}^{\mathfrak{g}}_{\mathfrak{m},(\widehat{\mathfrak{pr}}^{\mathfrak{g}}_{\mathfrak{m}},\hat{e}^{\mathfrak{g}}_{\mathfrak{m}})}\right) = -1 \\ 1 & if\ sign\left(\mathcal{Z}^{\mathfrak{g}}_{\mathfrak{m},(\widehat{\mathfrak{pr}}^{\mathfrak{g}}_{\mathfrak{m}},\hat{e}^{\mathfrak{g}}_{\mathfrak{m}})}\right) = +1 \end{cases} \tag{6}$$

When using the GSPIM-DCSKII method, the permuted version of the reference sequence distributes one bit to each effective carrier in the $\mathfrak{g}^{th}$ block. The $\mathfrak{p}1$ bits are used by each block to determine whether of the $2^{\mathfrak{p}1}$ carriers is unoccupied. The block's total number of bits broadcast is $(\mathfrak{p}1 + (2^{\mathfrak{p}1} - 1)(\mathfrak{p}2 + 1))$ bits, while the technique's total number is $G(\mathfrak{p}1 + (2^{\mathfrak{p}1} - 1)(\mathfrak{p}2 + 1))$ bits. The symbols for the modulated bits and permutations are $(2^{\mathfrak{p}1} - 1)$ and $\mathfrak{p}2(2^{\mathfrak{p}1} - 1)$. Equations (2) and (3) explain the waves that are broadcast and received respectively. Both transmitter and receiver unit designs may be used to define the transceiver structure for the GSPIM-DCSKII system. Finding the index of the non-active carrier in the $\mathfrak{g}^{th}$ block requires determining the greatest value of correlation matrices $\boldsymbol{\mathcal{Z}}^{\mathfrak{g}}_{\mathfrak{m}}$ for each carrier $\mathfrak{r}$, $\mathfrak{r}$ =1,…, $2^{\mathfrak{p}1}, \mathfrak{g}$ =1,.., G. For every carrier, the greatest value is denoted as $\hat{\mathcal{Z}}^{\mathfrak{g}}_{\mathfrak{m},(\mathfrak{w}',\mathfrak{r})}$ $\mathfrak{r} = 1, \dots, 2^{\mathfrak{p}1}, \mathfrak{w}' = 1,2$. The passive carrier index, $\widehat{m}^{\mathfrak{g}}_{\mathfrak{m}}$, is calculated by taking the minimum of the biggest magnitude values and expressed using the subsequent formula:

$$\begin{bmatrix} \hat{\mathcal{Z}}^{\mathfrak{g}}_{\mathfrak{m},(1,\mathfrak{r})} \\ \hat{\mathcal{Z}}^{\mathfrak{g}}_{\mathfrak{m},(2,\mathfrak{r})} \end{bmatrix} = \arg \max_{\mathfrak{w}=1,..,2^{\mathfrak{p}2}} \left(\left|\mathcal{Z}^{\mathfrak{g}}_{\mathfrak{m},(\mathfrak{w},\mathfrak{r})}\right|\right) \tag{7}$$

$$\widehat{m}^{\mathfrak{g}}_{\mathfrak{m}} = \arg \min_{\mathfrak{r}=1,..,2^{\mathfrak{p}1}} \left(\left|\hat{\mathcal{Z}}^{\mathfrak{g}}_{\mathfrak{m},(1,\mathfrak{r})}\right|\right) \tag{8}$$

The modulated bit for the $\mathfrak{r}^{th}$ carrier in the g^th block, represented as $\hat{\mathfrak{a}}^{\mathfrak{g}}_{\mathfrak{m},\mathfrak{r}}$, and the $(2^{\mathfrak{p}1} - 1)(\mathfrak{p}2)$permutation mapped bit indexes, marked as $\widehat{\mathfrak{pr}}^{\mathfrak{g}}_{\mathfrak{m},\mathfrak{r}}$, are represented by the indexes $\hat{\mathcal{Z}}^{\mathfrak{g}}_{\mathfrak{m},(2,\mathfrak{r})}$ as:

$$\widehat{\mathfrak{pr}}^{\mathfrak{g}}_{\mathfrak{m},\mathfrak{r}} = \hat{\mathcal{Z}}^{\mathfrak{g}}_{\mathfrak{m},(2,\mathfrak{r})} \quad \mathfrak{r} = 1, \dots, 2^{\mathfrak{p}1}, \mathfrak{r} \neq \widehat{m}^{\mathfrak{g}}_{\mathfrak{m}} \tag{9}$$

$$\hat{\mathfrak{a}}^{\mathfrak{g}}_{\mathfrak{m},\mathfrak{r}} = \begin{cases} 0 & if\ sign\left(\hat{\mathcal{Z}}^{\mathfrak{g}}_{\mathfrak{m},(1,\widehat{\mathfrak{pr}}^{\mathfrak{g}}_{\mathfrak{m},\mathfrak{r}})}\right) = -1 \\ 1 & if\ sign\left(\hat{\mathcal{Z}}^{\mathfrak{g}}_{\mathfrak{m},(1,\widehat{\mathfrak{pr}}^{\mathfrak{g}}_{\mathfrak{m},\mathfrak{r}})}\right) = +1 \end{cases} \quad \begin{matrix} \mathfrak{g} = 1,.., G \\ \mathfrak{r} = 1,.., 2^{\mathfrak{p}1},\ \mathfrak{r} \neq \widehat{m}^{\mathfrak{g}}_{\mathfrak{m}} \end{matrix} \tag{10}$$

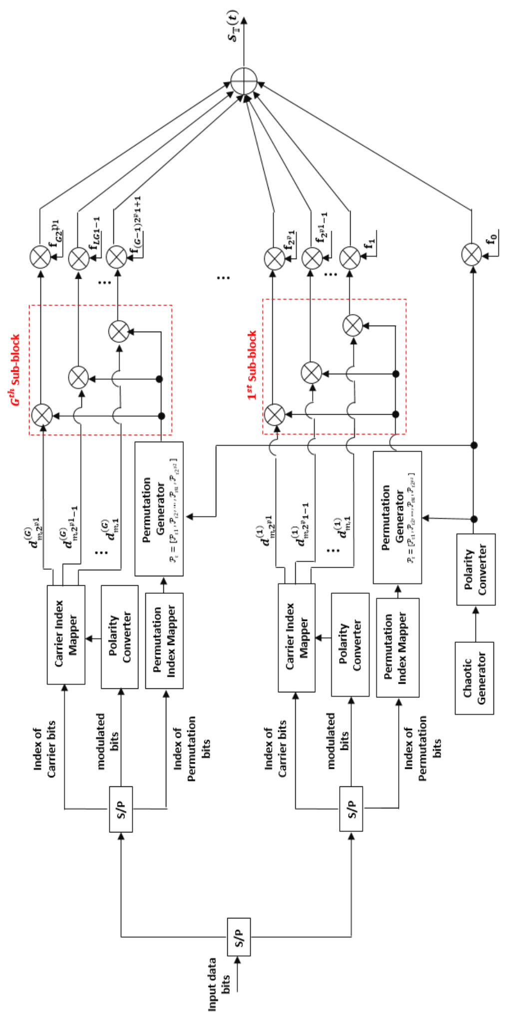

Figure 1. GSPIM-DCSK design's transmitter side unit arrangement.

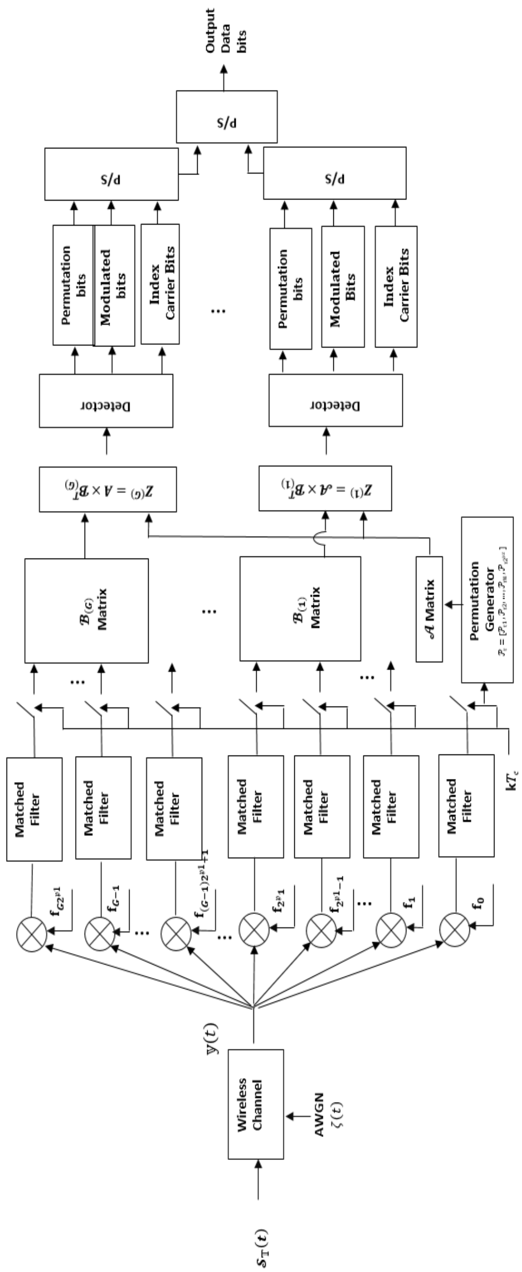

Figure 2. The GSPIM-DCSK design's receiver side unit arrangement.

3. A Novel Multi-Relay Two-Way Cooperative Network for Multiple Users using GSPIM-DCSK

In this part, a multiple-user cooperative system employing the GSPIM-DCSK techniques (GSPIM-DCSKI and GSPIM-DCSKII) is presented enabling 2-way, semi-duplex interaction among two and three clients through two relays. Users can communicate without being connected directly due to the relays that help with information transfer.

3.1. Two-user cooperative network based on multi-relay GSPIM-DCSK:

Two users ($\mathbb{U}1$ and $\mathbb{U}2$) and two relays ($\mathbb{R}1$ *and* $\mathbb{R}2$), each with one antenna, constitute this network. To achieve optimal effectiveness, the network employs the GSPIM-DCSK technique. Users $\mathbb{U}1$ and $\mathbb{U}2$ broadcast their information bits to the relays during distinct time periods, T1 and T2, so as to minimize disruption. Every relay node uses the protocol method known as Decode and Forward (DF). Broadcasting and relaying are the two steps that construct the communication channel. Figure 3 illustrates the two-step broadcasting and relaying architecture of the cooperative network based on multi-relay GSPIM-DCSK. $\mathcal{S}_{\mathbb{T}_{i,k}}$ indicates the signal delivered from users $\mathbb{U}i$ $(\mathrm{i} \in \{1,2\})$to relay $\mathbb{R}_k$ $(\mathrm{k} \in \{1,2\})$. This signal is identical to that in (2), except instead of $d_{\mathrm{m,r}}^{\mathbb{g}}$ and x_{m}, the parameters $d_{\mathrm{m,r},i}^{\mathbb{g},k}$ and $x_{\mathrm{m},u}$. The signal from users $\mathbb{U}i$ $(\mathrm{i} \in \{1,2\})$ is received by the relay node $\mathbb{R}_k$ $(\mathrm{k} \in \{1,2\})$ via $\mathbb{J}_{i,k}$ distinct routes of the Rayleigh distribution. This may be represented as follows.

$$y_{i,k}(t) = \sum_{\mathbb{j}=1}^{\mathbb{J}_{i,k}} \lambda_{i,k}^{\mathbb{j}} \delta(t - \tau_{i,k}^{\mathbb{j}}) \otimes \mathcal{S}_{\mathbb{T}_{i,k}}(t) + \zeta_{i,k}(t) \quad (11)$$

where $\zeta_{i,k}(t)$ indicates the AWGN for the connection from $\mathbb{U}i$ to $\mathbb{R}_k$, and $\lambda_{i,k}^{\mathbb{j}}$ and $\tau_{i,k}^{\mathbb{j}}$ signify the fading coefficient and the latency of the $\mathbb{j}^{th}$ path. The GSPIM-DCSK (GSPIM-DCSKI, GSPIM-DCSKII) demodulation is used by the relay nodes $\mathbb{R}_k$ $(k \in \{1,2\})$ to decode the data provided by the two users. When the GSPIM-DCSKI modulation scheme is used at the relay nodes and for each $\mathbb{g}^{th}$ sub-block, the formula in "Eq.4" is first used to determine the largest magnitude value ($\mathcal{Z}_{\mathrm{m},(\mathbb{u},\mathrm{r})}^{\mathbb{g},i,k}$) for each user at each relay. The lowest of the greatest magnitude values ($\hat{m}_{\mathrm{m},i,k}^{\mathbb{g}}$) for each user at each relay is first determined using the same method in (8) in the case of utilizing the GSPIM-DCSKII modulation scheme in the relay nodes and for each sub-block $\mathbb{g}$ =1,.., G. In order to keep things simple, ($\mathcal{Z}_{\mathrm{m},(\mathbb{u},\mathrm{r})}^{\mathbb{g},i,k}$) and ($\hat{m}_{\mathrm{m},i,k}^{\mathbb{g}}$) are expressed as $\mathcal{X}_{i,k}$,which is the reliability indicator for the active and inactive carriers in each sub-block of the GSPIM-DCSKI and GSPIM-DCSKII schemes, respectively, and can be expressed as follows:

$$\mathcal{X}^{\mathbb{g}}{}_{i,k} = \begin{cases} \mathcal{Z}_{\mathrm{m},(\mathbb{u},\mathrm{r})}^{\mathbb{g},i,k} & for\ relay\ wirh\ GSPIM-DCSKI\ scheme \\ \hat{m}_{\mathrm{m},i,k}^{\mathbb{g}} & for\ relay\ wirh\ GSPIM-DCSKII\ schem \end{cases} \quad (12)$$

Then, for each system sub-block, the following three relay-selection techniques are developed (Cai et al., 2017):

- Max-Sum (M_S^{g}) Relay-Selection

Two indicators, $M_S^{g}1$=$\mathcal{X}^{g}{}_{1,1}$ +$\mathcal{X}^{g}{}_{2,1}$ and $M_S^{g}2$=$\mathcal{X}^{g}{}_{1,2}$ +$\mathcal{X}^{g}{}_{2,2}$ are utilized in the M_S^{g} relay selection process to decide which relay should be chosen. We define the max-sum choosing procedure as follows:

$$\mathbb{R}^{g}{}_k = \arg\max_{k=1,2}\left(M_S^{g}n\right) \tag{13}$$

- Max-Product (M_P^{g}) Relay Selection:

The parameters $M_P^{g}1$=$\mathcal{X}^{g}{}_{1,1} \times \mathcal{X}^{g}{}_{2,1}$ and $M_P^{g}2$=$\mathcal{X}^{g}{}_{1,2} \times \mathcal{X}^{g}$ gar were employed for deciding which relay should be chosen in the M_P^{g} relay decision. The definition of the max-product choosing approach is:

$$\mathbb{R}^{g}{}_k = \arg\max_{k=1,2}\left(M_P^{g}n\right) \tag{14}$$

- Max-Min (M_M^{g})Relay Selection:

$M_M^{g}1$=$Min\{\mathcal{X}^{g}{}_{1,1},\mathcal{X}_{2,1}\}$ and $M_M^{g}2$=$Min\{\mathcal{X}^{g}{}_{1,2}$,$\mathcal{X}^{g}{}_{2,2}\}$ are utilized in the M_M^{g} relay selection to decide which relay should be chosen. The definition of the max-min choosing procedure is:

$$\mathbb{R}^{g}{}_k = \arg\max_{k=1,2}\left(M_M^{g}n\right) \tag{15}$$

In the decision-making process, $\mathbb{R}^{g}{}_1$ is chosen if $M^{g}1 \geq M^{g}2$, where $M_k \in \{M_S^{g}k, M_P^{g}k, M_M^{g}k\}\ and\ k \in \{1,2\}$. If not, $\mathbb{R}^{g}{}_2$is chosen. Subsequently, at every sub-block, the designated relay node employed the XOR functioning, as indicated by $\oplus$, to combine the signals obtained from users 1 and 2 ($\widehat{\mathcal{S}^{g}_{\mathbb{m},1,k}}$, $\widehat{\mathcal{S}^{g}_{\mathbb{m},2,k}}$,) to generate network-coded bits of data ($\mathcal{S}^{g}_{\mathbb{m},c}$) . These bits were subsequently transmitted to the central unit, which gathered the network-coded information bits from every sub-block. The goal was to distribute these bits, via the relaying phase, to every subscriber in just one slot, utilizing the GSPIM-DCSK (GSPIM-DCSKI, GSPIM-DCSKII) modulation framework. To sum up, the two phases have a total of three-time slots, or $\mathbb{T} = 3\beta T_c$ in duration. Moreover, $\mathcal{S}_{\mathbb{T}}c(t)$ provides the signals that the center unit transmitted to the two users; this is equivalent to "Eq.2", but the parameters are $x_{\mathbb{m},c}$and $d^{g,c}_{\mathbb{m},\mathbb{r}}$ rather than $d^{g}_{\mathbb{m},\mathbb{r}}$ and $x_{\mathbb{m}}$, respectively. User1 and User2's signals from the relay along $\mathbb{J}_{c,i}$ distinct routes of the Rayleigh distribution may be represented by the following:

$$\mathbb{y}_{c,i}(t) = \sum_{\mathbb{j}=1}^{\mathbb{J}_{c,i}} \lambda^{\mathbb{j}}_{c,i}\,\delta(t - \tau^{\mathbb{j}}_{c,i}) \otimes \mathcal{S}_{\mathbb{T}_c}(t) + \zeta_{c,i}(t) \tag{16}$$

The parameters of the $\mathbb{j}^{th}$ link for the center unit are represented as $\lambda^{\mathbb{j}}_{c,i}$ for users 1 and 2, while $\zeta_{c,i}(t)$denotes the AWGN. At user 1, the self-information bit and the observed data bits $\widehat{\mathcal{S}_{\mathbb{m},c}}$ from the center unit will be combined to find the user 2 data bits. Specifically, the self-information bit for user 1 and the recognized data bits from the center unit will be XORed to obtain the anticipated data bits for user 2, which are expressed as follows:

$$\widehat{\mathcal{S}_{\mathbb{m},2}} = \widehat{\mathcal{S}_{\mathbb{m},c}} \oplus \mathcal{S}_{\mathbb{m},1} \tag{17}$$

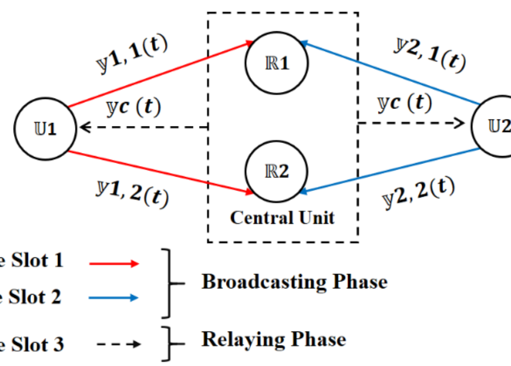

Figure 3. GSPIM-DCSK modulation scheme-based multi-relay cooperative system with two users

3.2. Three-user cooperative network based on multi-relay GSPIM-DCSK

There are two relays ($\mathbb{R}1\ and\ \mathbb{R}2$) and three-users ($\mathbb{U}1$, $\mathbb{U}2$, and $\mathbb{U}3$) in this network. There is one antenna per node. The cooperative relaying infrastructure's terminals are outfitted with the GSPIM-DCSK scheme, which comes in two variations: GSPIM-DCSKI and GSPIM-DCSKII, to enhance network functioning. To prevent disruptions, the three-users send their information bits to the relays ($\mathbb{R}1\ and\ \mathbb{R}2$) at different periods ($\mathbb{T}1$, $\mathbb{T}2$, and $\mathbb{T}3$). In the network, the relay point uses the Decode and Forward (DF) protocol. The relaying phase and the broadcasting procedure are required to establish a communication link between the users. Figure 4 depicts the overall architecture of the proposed GSPIM-DCSK cooperative network. The signal delivered to the relay $\mathbb{R}_k$ (k $\in$ {1,2}) from users $\mathbb{U}i$ (i $\in$ {1,2,3}) is represented by $\mathcal{S}_{\mathbb{T}_{i,k}}$, which is identical to "Eq.2" but uses $x_{\mathbb{m},u}$ and $d^{g,k}_{\mathbb{m},\mathbb{r},i}$as parameters rather than $d^{g}_{\mathbb{m},\mathbb{r}}$ and $x_{\mathbb{m}}$, respectively. Relays nodes $\mathbb{R}_k$ (k $\in$ {1,2}) employ GSPIM-DCSK demodulation to decode data sent by the three-users via $\mathbb{J}_{i,k}$ different paths of the Rayleigh distribution. These data are comparable to "Eq.11". The GSPIM-DCSKI modulation method uses the formula in "Eq.4" to determine the maximum magnitude value ($\mathcal{Z}^{\mathbb{g},i,k}_{\mathfrak{m},(\mathbb{u},\mathfrak{r})}$) for each user at each relay for each $\mathbb{g}^{th}$ sub-block. On the other hand, the GSPIM-DCSKII modulation scheme uses the same method in "Eq.8" to get the minimum of the greatest magnitude values ($\widehat{m}^{\mathbb{g}}_{\mathfrak{m},i,k}$) for each user at each relay. ($\mathcal{Z}^{\mathbb{g},i,k}_{\mathfrak{m},(\mathbb{u},\mathfrak{r})}$) and ($\widehat{m}^{\mathbb{g}}_{\mathfrak{m},i,k}$) are expressed simply as $\mathcal{X}_{i,k}$, which may be expressed as "Eq.12". This indicates the dependability of the active and inactive carriers in each sub-block of the GSPIM-DCSKI and GSPIM-DCSKII schemes, respectively. For every system sub-block, the following three relay-selection techniques are developed :

- Max-Sum ($M^{\mathbb{g}}_S k, n$) Relay Selection

Four parameters are employed in the $M^{\mathbb{g}}_S k, n$ relay selection process to choose the relay that will send data to every user during the first and second relaying phases, where $n \in \{1, 2\}$. The relay node for $\mathbb{U}1, \mathbb{U}2$ is selected using $M^{\mathbb{g}}_S 1{,}1$=$\mathcal{X}^{\mathbb{g}}{}_{1,1}$ +$\mathcal{X}^{\mathbb{g}}{}_{2,1}$ and $M^{\mathbb{g}}_S 2{,}1$=$\mathcal{X}^{\mathbb{g}}{}_{1,2}$ +$\mathcal{X}^{\mathbb{g}}{}_{2,2}$ and for $\mathbb{U}1, \mathbb{U}3$, the relay node is selected using $M^{\mathbb{g}}_S 1{,}2$=$\mathcal{X}^{\mathbb{g}}{}_{1,1}$ +$\mathcal{X}^{\mathbb{g}}{}_{3,1}$ and $M^{\mathbb{g}}_S 2{,}2$=$\mathcal{X}^{\mathbb{g}}{}_{1,2}$ +$\mathcal{X}^{\mathbb{g}}{}_{3,2}$. The definition of the max-sum choosing process is:

The selected relay node for $\mathbb{U}1, \mathbb{U}2$:

$$\mathbb{R}^{\mathbb{g}}{}_k = \arg \max_{k=1,2,n=1} \left(M^{\mathbb{g}}_S k, 1\right) \tag{18}$$

The selected relay node for $\mathbb{U}1, \mathbb{U}3$:

$$\mathbb{R}^{\mathbb{g}}{}_k = \arg \max_{k=1,2,n=2} \left(M^{\mathbb{g}}_S k, 2\right) \tag{19}$$

- Max-Product ($M^{\mathbb{g}}_P k, n$) Relay Selection:

Four indicators are utilized in the $M^{\mathbb{g}}_{P,n}$ relay selection process to evaluate which relay should be chosen. The relay node for $\mathbb{U}1, \mathbb{U}2$ is selected using $M^{\mathbb{g}}_P 1{,}1$=$\mathcal{X}^{\mathbb{g}}{}_{1,1} \times \mathcal{X}^{\mathbb{g}}{}_{2,1}$ and $M^{\mathbb{g}}_P 2{,}1$=$\mathcal{X}^{\mathbb{g}}{}_{1,2} \times \mathcal{X}^{\mathbb{g}}{}_{2,2}$; the relay node for $\mathbb{U}1, \mathbb{U}3$ is selected using $M^{\mathbb{g}}_P 1{,}2$=$\mathcal{X}^{\mathbb{g}}{}_{1,1} \times \mathcal{X}^{\mathbb{g}}{}_{3,1}$ and $M^{\mathbb{g}}_P 2{,}2$=$\mathcal{X}^{\mathbb{g}}{}_{1,2} \times \mathcal{X}^{\mathbb{g}}{}_{3,2}$. The definition of the max-product choosing approach is:

The selected relay node for $\mathbb{U}1, \mathbb{U}2$:

$$\mathbb{R}^{\mathbb{g}}{}_k = \arg \max_{k=1,2,n=1} \left(M^{\mathbb{g}}_P k, 1\right) \tag{20}$$

The selected relay node for $\mathbb{U}1, \mathbb{U}3$:

$$\mathbb{R}^{\mathbb{g}}{}_k = \arg \max_{k=1,2,n=2} \left(M^{\mathbb{g}}_P k, 2\right) \tag{21}$$

Max-Min ($M^{\mathbb{g}}_M k, n$) Relay Selection:

$M^{\mathbb{g}}_M 1{,}1$=$Min\{\mathcal{X}^{\mathbb{g}}{}_{1,1}, \mathcal{X}_{2,1}\}$ and $M^{\mathbb{g}}_M 2{,}1$=$Min\{\mathcal{X}^{\mathbb{g}}{}_{1,2}, \mathcal{X}^{\mathbb{g}}{}_{2,2}\}$ are used in the $M^{\mathbb{g}}_{M,n}$ relay choice procedure to decide which relay to be picked for $\mathbb{U}1, \mathbb{U}2$, and $M^{\mathbb{g}}_M 1{,}2$=$Min\{\mathcal{X}^{\mathbb{g}}{}_{1,1}, \mathcal{X}_{3,1}\}$ and $M^{\mathbb{g}}_M 2{,}2$=$Min\{\mathcal{X}^{\mathbb{g}}{}_{1,2}, \mathcal{X}^{\mathbb{g}}{}_{3,2}\}$ are used for deciding which relay to be picked for $\mathbb{U}1, \mathbb{U}3$. The definition of the max-min choosing policy is:

The selected relay node for $\mathbb{U}1, \mathbb{U}2$:

$$\mathbb{R}^{\mathbb{g}}{}_k = \arg \max_{k=1,2,n=1} \left(M^{\mathbb{g}}_M k, 1\right) \tag{22}$$

The selected relay node for $\mathbb{U}1, \mathbb{U}3$:

$$\mathbb{R}^{\mathbb{g}}{}_k = \arg \max_{k=1,2,n=2} \left(M^{\mathbb{g}}_M k, 2\right) \tag{23}$$

The choosing procedure is as follows: if if $M^{\mathbb{g}}1{,}1 \geq M^{\mathbb{g}}2{,}1$, and if $M^{\mathbb{g}}1{,}2 \geq M^{\mathbb{g}}2{,}2$, where $M_{k,n} \in \left\{M^{\mathbb{g}}_S k, M^{\mathbb{g}}_P k, M^{\mathbb{g}}_M k\right\}, k \in \{1, 2\}$,and $n \in \{1, 2\}$, then $\mathbb{R}^{\mathbb{g}}{}_1$ is chosen; if not, $\mathbb{R}^{\mathbb{g}}{}_2$ is selected. As (($\widehat{\mathcal{S}_{\mathfrak{m},1,\mathrm{k}}}$, $\widehat{\mathcal{S}_{\mathfrak{m},2,\mathrm{k}}}$ and $\widehat{\mathcal{S}_{\mathfrak{m},3,\mathrm{k})}}$, the data broadcasted by the three-users and decoded by the relay node may be represented. Using the XOR technique displayed by $\oplus$, the chosen relay node combines the signals from users 1 and 2 and users 1 and 3 to generate two network-coded bits of information ($\mathcal{S}^{\mathbb{g}}_{\mathfrak{m},c,1}$ and $\mathcal{S}^{\mathbb{g}}_{\mathfrak{m},c,2}$). These bits are subsequently transmitted to the central unit to gather the network-coded data bits from every sub-block so that they can be delivered to both users in a two-time slot through the two relaying phases using GSPIM-DCSK (GSPIM-DCSKI, GSPIM-DCSKII) modulation scheme. $\mathbb{T} = 5\beta T_c$ is the entire duration of the two phases, which together include five- time slots. Moreover, $\mathcal{S}_{\mathbb{T}}c, 1(t)$ and $\mathcal{S}_{\mathbb{T}}c, 2(t)$ indicate the signals that the center unit delivered to the three-users at the first and second relaying periods, respectively. These are identical to "Eq.2", but at the first relaying phase, the parameters are $d^{\mathbb{g},c,1}_{\mathfrak{m},\mathfrak{r}}$ and $x_{\mathfrak{m},c,1}$, and at the second relaying phase, they are $d^{\mathbb{g},c,2}_{\mathfrak{m},\mathfrak{r}}$ and $x_{\mathfrak{m},c,2}$, rather than $d^{\mathbb{g}}_{\mathfrak{m},\mathfrak{r}}$ and $x_{\mathfrak{m}}$. The signals received by the three-users via $\mathbb{J}_{c,i}$ different paths of the Rayleigh distribution from the center unit during the first and second relaying periods are represented by the following:

$$\mathbb{y}_{c,1,i}(t) = \sum_{\mathbb{j}=1}^{\mathbb{J}_{c,1,i}} \lambda^{\mathbb{j}}_{c,1,i} \delta(t - \tau^{\mathbb{j}}_{c,1,i}) \otimes \mathcal{S}_{\mathbb{T}_{c,1}}(t) + \zeta_{c,1,i}(t) \tag{24}$$

$$\mathbb{y}_{c,2,i}(t) = \sum_{\mathbb{j}=1}^{\mathbb{J}_{c,2,i}} \lambda^{\mathbb{j}}_{c,2,i} \delta(t - \tau^{\mathbb{j}}_{c,2,i}) \otimes \mathcal{S}_{\mathbb{T}_{c,2}}(t) + \zeta_{c,2,i}(t) \tag{25}$$

The parameters of the relay in the first and second-time slots for each of the three users are represented by $\lambda_{\mathbb{j},c,1,i}$ and $\lambda_{\mathbb{j},c,2,i}$ for the $\mathbb{j}^{th}$ link.Both $\zeta_{c,1,i}(t)$ and $\zeta_{c,2,i}(t)$show AWGN. The self-data bit will be combined with the observed data bits ($\widehat{\mathcal{S}_{\mathbb{m},c,1}}$, and $\widehat{\mathcal{S}_{\mathbb{m},c,2}}$) obtained from the center unit at $\mathbb{U}1$ to identify the data bits of $\mathbb{U}2$ and $\mathbb{U}3$ at $\mathbb{U}1$. More specifically, the information bits from the center unit and the personal data bit at user 1 will be XORed to create the estimated information bits for $\mathbb{U}2$ and $\mathbb{U}3$, which are as follows:

$$\widehat{\mathcal{S}_{\mathbb{m},2}} = \widehat{\mathcal{S}_{\mathbb{m},c,1}} \oplus \mathcal{S}_{\mathbb{m},1} \tag{26}$$

$$\widehat{\mathcal{S}_{\mathbb{m},3}} = \widehat{\mathcal{S}_{\mathbb{m},c,2}} \oplus \mathcal{S}_{\mathbb{m},1} \tag{27}$$

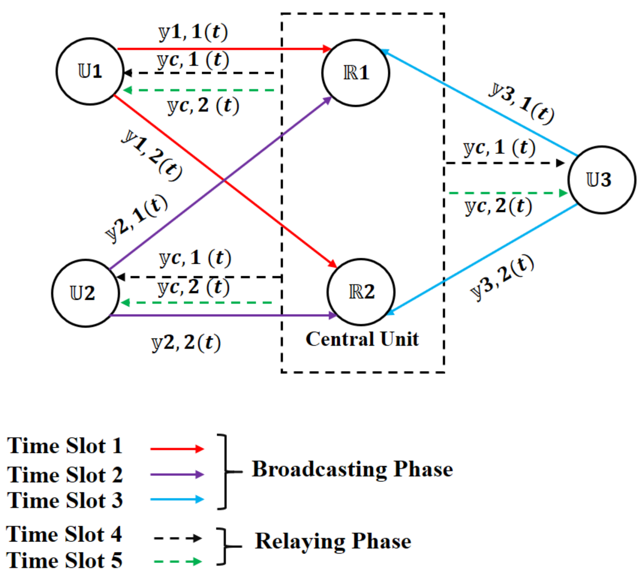

Figure 4. GSPIM-DCSK modulation scheme-based multi-relay cooperative system with three-users.

4. Results of Simulation Achievement and Discussions:

Under the influence of three routes of Rayleigh fading channels, the BER performances for the proposed Multi-Relay Multiuser Cooperative network based on GSPIM-DCSKI and GSPIM-DCSKII systems are provided in this section. Additionally, these systems' performance comparisons with single relay two and three-users cooperative networks based on two different types of GSIM-DCSK and DCSK systems are presented. Table 1 and Table 2, respectively, provide the average power gain and delay time for each route of the Rayleigh fading channel.

The total number of sub-carriers and mapping bits (carrier and permutation indices) that were ultimately selected for the Multi-Relay Two-way Multi-users cooperative-based GSPIM-DCSK with its two distinct variants (GSPIM-DCSKI and GSPIM-DCSKII) structures with spreading factor β=128 is equal to ($\mathfrak{p}$ =6, 2^6+1=65), $\mathfrak{p}1$ =2, and $\mathfrak{p}2$=2, respectively. Figures 5 and 6 illustrate how the average bit error rate performance of single relay two-user cooperative systems using two types of GSPIM-DCSK and DCSK systems is compared to that of two relay two-way two-user cooperative networks using GSPIM-DCSKI and GSPIM-DCSKII with Max-Product, Max-Minimum, and Max-Sum relay selection algorithms.

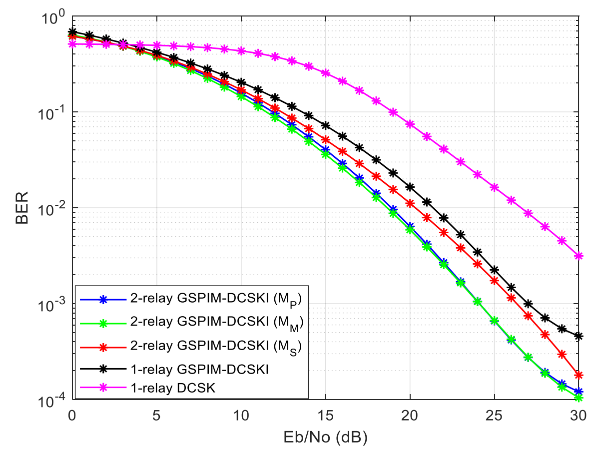

Figure 5. Two relay two-users cooperative networking based on GSPIM-DCSKI along with other cooperative platforms are contrasted for average BER.

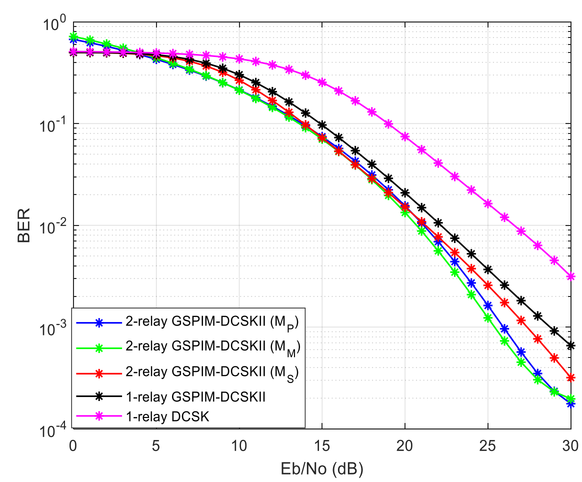

Figure 6. Two relay two-users cooperative networking based on GSPIM-DCSKII along with other cooperative platforms are contrasted for average BER.

Table 1. System parameters for two-relay two-user cooperative system.

Nodes	Average Power Gain			Chips Time Delays		
$\mathbb{U}1$ to $\mathbb{R}_1$	$E\left(\lambda^2_{1,\mathbb{U}1\to\mathbb{R}_1}\right)$	$E\left(\lambda^2_{2,\mathbb{U}1\to\mathbb{R}_1}\right)$	$E\left(\lambda^2_{3,\mathbb{U}1\to\mathbb{R}_1}\right)$	$\tau_{1,\mathbb{U}1\to\mathbb{R}_1}$	$\tau_{2,\mathbb{U}1\to\mathbb{R}_1}$	$\tau_{3,\mathbb{U}1\to\mathbb{R}_1}$
	1/3	1/3	1/3	0	2	5
	$E\left(\lambda^2_{1,\mathbb{U}1\to\mathbb{R}_2}\right)$	$E\left(\lambda^2_{2,\mathbb{U}1\to\mathbb{R}_2}\right)$	$E\left(\lambda^2_{3,\mathbb{U}1\to\mathbb{R}_2}\right)$	$\tau_{1,\mathbb{U}1\to\mathbb{R}_2}$	$\tau_{2,\mathbb{U}1\to\mathbb{R}_2}$	$\tau_{3,\mathbb{U}1\to\mathbb{R}_1}$
	1/2	2/5	1/10	0	1	4
$\mathbb{U}2$ to $\mathbb{R}_k$	$E\left(\lambda^2_{1,\mathbb{U}2\to\mathbb{R}_1}\right)$	$E\left(\lambda^2_{2,\mathbb{U}2\to\mathbb{R}_1}\right)$	$E\left(\lambda^2_{3,\mathbb{U}2\to\mathbb{R}_1}\right)$	$\tau_{1,\mathbb{U}2\to\mathbb{R}_1}$	$\tau_{2,\mathbb{U}2\to\mathbb{R}_1}$	$\tau_{3,\mathbb{U}2\to\mathbb{R}_1}$
	1/10	2/5	1/2	0	3	6
	$E\left(\lambda^2_{1,\mathbb{U}2\to\mathbb{R}_2}\right)$	$E\left(\lambda^2_{2,\mathbb{U}2\to\mathbb{R}_2}\right)$	$E\left(\lambda^2_{3,\mathbb{U}2\to\mathbb{R}_2}\right)$	$\tau_{1,\mathbb{U}2\to\mathbb{R}_2}$	$\tau_{2,\mathbb{U}2\to\mathbb{R}_2}$	$\tau_{3,\mathbb{U}2\to\mathbb{R}_2}$
	2/5	1/10	1/2	0	4	8
$\mathbb{C}$ to $\mathbb{U}1$ & $\mathbb{U}2$	$E\left(\lambda^2_{1,\mathbb{C}\to\mathbb{U}}\right)$	$E\left(\lambda^2_{2,\mathbb{C}\to\mathbb{U}}\right)$	$E\left(\lambda^2_{3,\mathbb{C}\to\mathbb{U}}\right)$	$\tau_{1,\mathbb{C}\to\mathbb{U}}$	$\tau_{2,\mathbb{C}\to\mathbb{U}}$	$\tau_{3,\mathbb{C}\to\mathbb{U}}$
	1/3	1/5	7/15	0	5	7

Table 2. System parameters for two-relay three-user cooperative system.

Nodes	Average Power Gain			Chips Time Delays		
$\mathbb{U}1$ to $\mathbb{R}_1$	$E\left(\lambda^2_{1,\mathbb{U}1\to\mathbb{R}_1}\right)$	$E\left(\lambda^2_{2,\mathbb{U}1\to\mathbb{R}_1}\right)$	$E\left(\lambda^2_{3,\mathbb{U}1\to\mathbb{R}_1}\right)$	$\tau_{1,\mathbb{U}1\to\mathbb{R}_1}$	$\tau_{2,\mathbb{U}1\to\mathbb{R}_1}$	$\tau_{3,\mathbb{U}1\to\mathbb{R}_1}$
	1/3	1/3	1/3	0	2	5
	$E\left(\lambda^2_{1,\mathbb{U}1\to\mathbb{R}_2}\right)$	$E\left(\lambda^2_{2,\mathbb{U}1\to\mathbb{R}_2}\right)$	$E\left(\lambda^2_{3,\mathbb{U}1\to\mathbb{R}_2}\right)$	$\tau_{1,\mathbb{U}1\to\mathbb{R}_2}$	$\tau_{2,\mathbb{U}1\to\mathbb{R}_2}$	$\tau_{3,\mathbb{U}1\to\mathbb{R}_1}$
	1/2	2/5	1/10	0	1	4
$\mathbb{U}2$ to $\mathbb{R}_k$	$E\left(\lambda^2_{1,\mathbb{U}2\to\mathbb{R}_1}\right)$	$E\left(\lambda^2_{2,\mathbb{U}2\to\mathbb{R}_1}\right)$	$E\left(\lambda^2_{3,\mathbb{U}2\to\mathbb{R}_1}\right)$	$\tau_{1,\mathbb{U}2\to\mathbb{R}_1}$	$\tau_{2,\mathbb{U}2\to\mathbb{R}_1}$	$\tau_{3,\mathbb{U}2\to\mathbb{R}_1}$
	1/10	2/5	1/2	0	3	6
	$E\left(\lambda^2_{1,\mathbb{U}2\to\mathbb{R}_2}\right)$	$E\left(\lambda^2_{2,\mathbb{U}2\to\mathbb{R}_2}\right)$	$E\left(\lambda^2_{3,\mathbb{U}2\to\mathbb{R}_2}\right)$	$\tau_{1,\mathbb{U}2\to\mathbb{R}_2}$	$\tau_{2,\mathbb{U}2\to\mathbb{R}_2}$	$\tau_{3,\mathbb{U}2\to\mathbb{R}_2}$
	$E\left(\lambda^2_{1,\mathbb{U}2\to\mathbb{R}_1}\right)$	$E\left(\lambda^2_{2,\mathbb{U}2\to\mathbb{R}_1}\right)$	$E\left(\lambda^2_{3,\mathbb{U}2\to\mathbb{R}_1}\right)$	$\tau_{1,\mathbb{U}2\to\mathbb{R}_1}$	$\tau_{2,\mathbb{U}2\to\mathbb{R}_1}$	$\tau_{3,\mathbb{U}2\to\mathbb{R}_1}$
$\mathbb{U}3$ to $\mathbb{R}_k$	$E\left(\lambda^2_{1,\mathbb{U}3\to\mathbb{R}_1}\right)$	$E\left(\lambda^2_{2,\mathbb{U}3\to\mathbb{R}_1}\right)$	$E\left(\lambda^2_{3,\mathbb{U}3\to\mathbb{R}_1}\right)$	$\tau_{1,\mathbb{U}3\to\mathbb{R}_1}$	$\tau_{2,\mathbb{U}3\to\mathbb{R}_1}$	$\tau_{3,\mathbb{U}3\to\mathbb{R}_1}$
	3/5	1/10	3/10	0	3	6
	$E\left(\lambda^2_{1,\mathbb{U}3\to\mathbb{R}_2}\right)$	$E\left(\lambda^2_{2,\mathbb{U}3\to\mathbb{R}_2}\right)$	$E\left(\lambda^2_{3,\mathbb{U}3\to\mathbb{R}_2}\right)$	$\tau_{1,\mathbb{U}3\to\mathbb{R}_2}$	$\tau_{2,\mathbb{U}3\to\mathbb{R}_2}$	$\tau_{3,\mathbb{U}3\to\mathbb{R}_2}$
	4/5	1/10	1/10	0	5	8
$\mathbb{C}$ to $\mathbb{U}1$, $\mathbb{U}2$ and $\mathbb{U}3$ at First Relaying Phase	$E\left(\lambda^2_{1,\mathbb{C},1\to\mathbb{U}}\right)$	$E\left(\lambda^2_{2,\mathbb{C},1\to\mathbb{U}}\right)$	$E\left(\lambda^2_{3,\mathbb{C},1\to\mathbb{U}}\right)$	$\tau_{1,\mathbb{C},1\to\mathbb{U}}$	$\tau_{2,\mathbb{C},1\to\mathbb{U}}$	$\tau_{3,\mathbb{C},1\to\mathbb{U}}$
	1/3	1/5	7/15	0	5	7
$\mathbb{C}$ to $\mathbb{U}1$, $\mathbb{U}2$ and $\mathbb{U}3$ at Second Relaying Phase	$E\left(\lambda^2_{1,\mathbb{C},2\to\mathbb{U}}\right)$	$E\left(\lambda^2_{2,\mathbb{C},2\to\mathbb{U}}\right)$	$E\left(\lambda^2_{3,\mathbb{C},2\to\mathbb{U}}\right)$	$\tau_{1,\mathbb{C},2\to\mathbb{U}}$	$\tau_{2,\mathbb{C},2\to\mathbb{U}}$	$\tau_{3,\mathbb{C},2\to\mathbb{U}}$
	1/5	2/15	2/3	0	3	8

It also contrasts the single relay three user cooperative system based on two types of GSPIM-DCSK and DCSK systems with the average bit error rate performance of two relay two-way three-user cooperative networks using GSPIM-DCSKI and GSPIM-DCSKII with Max-Product, Max-Minimum, and Max-Sum relay selection algorithms, as shown in Figures 7 and 8. These figures show that the cooperative system with the relay selection algorithm performs better than the other systems that just have one relay. Whereas the cooperative system based on GSPIM-DCSKI for two users obtained SNR about 4 dB with Max-Product, Max-Minimum relay choosing technique, and 0.5 dB with Max-Sum relay choosing technique at average BER = 10^{-3} compared to the cooperative system based on GSPIM-DCSKI with just one relay, and at average BER = 10^{-2} obtained SNR about 7.5 dB with Max-Product, Max-Minimum relay choosing technique, and 6.5 dB with Max-Sum relay choosing technique compared to the cooperative system based on DCSK scheme, as Figure 5 displays. Additionally, the two-user cooperative system based on GSPIM-DCSKII gained SNR of about 4 dB with the Max-Product, Max-Minimum, and 1 dB with the Max-Sum relay choice techniques at average BER = 10^{-3} compared to the cooperative system based on GSPIM-DCSKII with a single relay and at BER = 10^{-2} gained SNR about 5 dB with relay choosing approaches compared to the cooperative system based on DCSK scheme, as shown in Figure 6. Figure 7 illustrates how the three-user cooperative system based on GSPIM-DCSKI increased SNR by approximately 3.2 dB with Max-Product, Max-Minimum relay selection method, and 2 dB with Max-Sum relay selection method compared to the three-user cooperative system based on GSPIM-DCSKI with single relay at average BER = 10^{-3} and against the three user cooperative systems based on DCSK scheme, at BER = 10^{-2} achieved SNR about 7dB with Max-Product, Max-Minimum relay choosing technique, and approximately 5.25 dB with Max-Sum relay selection method. Additionally, the three-user cooperative system based on GSPIM-DCSKII gained SNR by approximately 3.5 dB with the Max-Product, Max-Minimum, and 1 dB with the Max-Sum relay choices at average BER = 10^{-3}compared to the cooperative system based on GSPIM-DCSKII with a single relay and at BER = 10^{-2} acquired SNR by approximately 5 dB with relay choosing techniques compared to the cooperative system based on DCSK scheme, as shown in Figure 8. Furthermore, of the three relay choosing techniques, the cooperative system utilizing the Max-Product and the Max-Minimum decisions based on the GSPIM-DCSKI scheme executes more effectively than the Max-Sum choosing, with an average BER = 10^{-3} for the systems based on the GSPIM-DCSKI with Max-Product and the Max-Minimum decisions obtained SNR by approximately 2 and 0.5 dB at two and three users, respectively, compared to the system with Max-Sum procedure as shown in Figure 5 and 7 respectively.

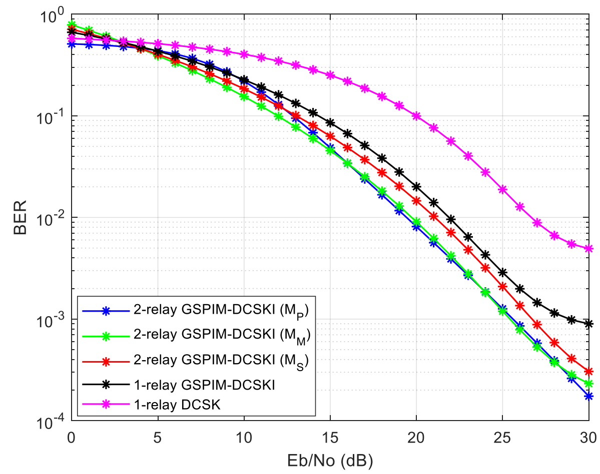

Figure 7: Two relay three-users cooperative networking based on GSPIM-DCSKI along with other cooperative platforms are contrasted for average BER.

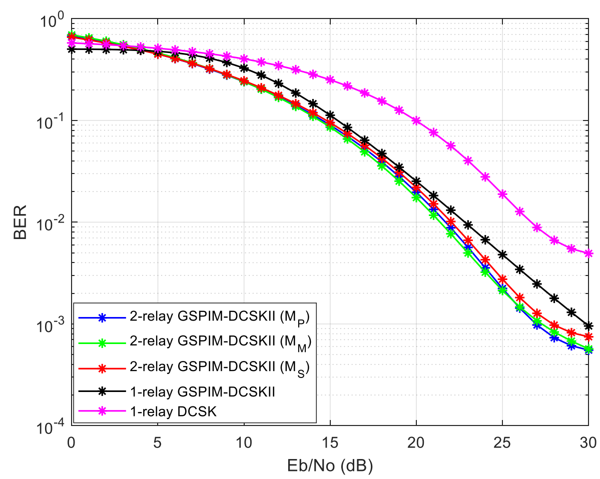

Figure 8. Two relay three-users cooperative networking based on GSPIM-DCSKII along with other cooperative platforms are contrasted for average BER.

The GSPIM-DCSKII cooperative system exhibits consistent performance up to SNR = 21 dB. Subsequently, the two and three-user systems with the Max-Product and Max-Minimum decisions exhibit comparable error performances and outperform the Max-Sum selection. At an average BER of 10^{-3}, the two and three-user systems based on GSPIM-DCSKII gained approximately 1 and 0.5 dB at the two and three-user, respectively, compared to the Max-Sum mechanism depicted in Figures 5 and 7, respectively. However, because the Max-Sum decision uses straightforward addition and comparison procedures, it has the least complexity. In addition, the GSPIM-DCSK cooperative system is a multi-carrier system that splits into groups which allow for the transmission of more information than the collaborative network based on DCSK at a single symbol length. In the cooperative structure based on GSPIM-DCSKI, every user passes 80 bits, whereas in the cooperative system based on GSPIM-DCSKII, 176 bits. The cooperative network based on the DCSK system delivers only a single bit, which results in the cooperative system based on DCSK scheme performing worse than other systems due to the fact that it consumes more energy to send just one bit from every customer. Moreover, the number of time slots that spent for the two phases of the cooperative process is different, where the two-user and three-user cooperative system based the two type of GSPIM-DCSK spend three-time slot equal to 3βT and five-time slot equal to 5βT respectively, while two and three-user cooperative network based DCSK system demands six and ten time slots respectively to complete the cooperation process.

5. Conclusion

This study proposes a unique Multi-Relay Two-Way Multi-User half-duplex cooperative network to enhance the error reliability of a Single-Relay Two-Way half-duplex cooperative communication network based on a GSPIM-DCSK. The design of this system is based on the Joint Grouping Subcarrier-Permutation Index Modulation-DCSK (GSPIM-DCSK) scheme. Although numerous relays are set up in this system, only one relay is used for supplying network-coded data to the clients during the relaying phase. It is projected that every relay node in this network makes use of the Decode and Forward (DF) protocol technique. Not all relays are employed, just one relay, which improves network performance overall and offers dependable communication between users is selected for transition. The max-sum (M_S), max-min (M_M), and max-product (M_P) relay techniques are the three that are employed for selection. The average BER performance of the novel system is evaluated by acquiring and applying the simulation findings at multipath Rayleigh fading channels. Furthermore, a comparative analysis is conducted between the two and three-users cooperative system-based DCSK and GSPIM-DCSK that utilizes a single relay and a novel cooperative-based GSPIM-DCSK system, with two and three users, that utilizes multiple relays. Simulation results show that the cooperative system with the relay selection algorithm performs better than the other systems that just have one relay. Furthermore, the cooperative system utilizing M_P and M_M decisions based on the GSPIM-DCSK scheme executes more effectively than the M_S choosing mechanism. However, because the M_S decision uses straightforward addition and comparison procedures, it has the least complexity. In addition, the GSPIM-DCSK cooperative system is a multi-carrier system which allow for the transmission of more information than the collaborative network based on DCSK at a single symbol length, which results in the cooperative system based on DCSK scheme performing worse than other systems due to the fact that it consumes more energy to send just one bit from every customer.

Conflict of interest

The authors have no conflict of interest to declare.

Funding

The authors received no specific funding for this work.

Acknowledgements

This work is supported by the College of Engineering/Mustansiriyah University (https://www.uomustansiriyah.edu.iq).

References

Aboltins, A., & Tihomorskis, N. (2023). Software-Defined radio implementation and performance evaluation of Frequency-Modulated Antipodal Chaos Shift Keying Communication System. Electronics, 12(5), 1240. https://doi.org/10.3390/electronics12051240

Bai, C., Ren, H., Baptista, M. S., & Grebogi, C. (2019). Digital underwater communication with chaos. Communications in Nonlinear Science and Numerical Simulation, 73, 14–24. https://doi.org/10.1016/j.cnsns.2019.01.027

Cai, G., Fang, Y., Han, G., Xu, J., & Chen, G. (2017). Design and Analysis of Relay-Selection Strategies for Two-Way Relay Network-Coded DCSK Systems. IEEE Transactions on Vehicular Technology, 67(2), 1258–1271. https://doi.org/10.1109/tvt.2017.2751754

Chen, Z., Zhang, L., Wang, W., & Wu, Z. (2021). A Pre-Coded Multi-CarrierM-Ary chaotic vector cyclic shift keying transceiver for reliable communications. IEEE Transactions on Wireless Communications, 21(2), 1007–1021. https://doi.org/10.1109/twc.2021.3100620

Cheng, G., Wang, L., Xu, W., & Chen, G. (2016). Carrier Index differential Chaos shift keying modulation. IEEE Transactions on Circuits & Systems II Express Briefs, 64(8), 907–911. https://doi.org/10.1109/tcsii.2016.2613093

Fang, Y., Chen, W., Chen, P., Tao, Y., & Guizani, M. (2022). SR-DCSK Cooperative Communication System with Code Index Modulation: A New Design for 6G New Radios. arXiv (Cornell University).
https://doi.org/10.48550/arxiv.2208.12970

Hasan, F. S. (2020). Design and analysis of Three-Way relay Network coding schemes based Differential Chaos Shift keying Communication System. Wireless Personal Communications, 114(1), 29–47.
https://doi.org/10.1007/s11277-020-07348-5

Hasan, F. S. (2021). Design and analysis of grouping subcarrier index modulation for differential chaos shift keying communication system. Physical Communication, 47, 101325.
https://doi.org/10.1016/j.phycom.2021.101325

Kaddoum, G. (2016). Wireless Chaos-Based Communication Systems: A Comprehensive survey. IEEE Access, 4, 2621–2648.
https://doi.org/10.1109/access.2016.2572730

Kaddoum, G., & El-Hajjar, M. (2015). Analysis of network coding schemes for differential chaos shift keying communication system. ArXiv Preprint ArXiv:1505.02851.
https://doi.org/10.48550/arXiv.1505.02851

Kaddoum, G., Richardson, F., & Gagnon, F. (2013). Design and Analysis of a Multi-Carrier Differential Chaos Shift keying Communication System. IEEE Transactions on Communications, 61(8), 3281–3291.
https://doi.org/10.1109/tcomm.2013.071013.130225

Lau, F., Cheong, K., & Tse, C. (2003). Permutation-based DCSK and multiple-access DCSK systems. IEEE Transactions on Circuits and Systems I Fundamental Theory and Applications, 50(6), 733–742.
https://doi.org/10.1109/tcsi.2003.812616

Li, S., Zhao, Y., & Wu, Z. (2015). Design and analysis of an OFDM-based differential Chaos Shift keying Communication System. Journal of Communications, 10(3), 199–205.
https://doi.org/10.12720/jcm.10.3.199-205

Nazar, B., & Hasan, F. S. (2023a). PERFORMANCE IMPROVEMENT OF TWO-WAY COOPERATIVE DCSK SYSTEM USING GROUPING SUBCARRIER-PERMUTATION INDEX MODULATION. Journal of Engineering and Sustainable Development, 26–37.
https://doi.org/10.31272/conf.6.3.3

Nazar, B., & Hasan, F. S. (2023b). Joint grouping subcarrier and permutation index modulations based differential chaos shift keying system. Physical Communication, 61, 102213.
https://doi.org/10.1016/j.phycom.2023.102213

Nazar, B., & Hasan, F. S. (2024a). Enhanced Two-Way Cooperative DCSK System via Grouping Subcarrier-Permutation Index modulation. In Lecture notes in electrical engineering (pp. 23–35).
https://doi.org/10.1007/978-981-97-0644-0_3

Nazar, B., & Hasan, F. S. (2024b). Performance analysis of two-way multi-users cooperative communication system based on GSPIM-DCSK scheme. AEU - International Journal of Electronics and Communications, 178, 155303.
https://doi.org/10.1016/j.aeue.2024.155303

Que, D. T., Quyen, N. X., & Hoang, T. M. (2021). Performance of Improved-DCSK system over land mobile satellite channel under effect of time-reversed chaotic sequences. Physical Communication, 47, 101342.
https://doi.org/10.1016/j.phycom.2021.101342

Rasool, M., & Belhaouari, S. B. (2023b). From Collatz Conjecture to chaos and hash function. Chaos Solitons & Fractals, 176, 114103.
https://doi.org/10.1016/j.chaos.2023.114103

Xu, W., Wang, L., & Chen, G. (2010). Performance of DCSK cooperative communication systems over multipath fading channels. IEEE Transactions on Circuits and Systems I Regular Papers, 58(1), 196–204.
https://doi.org/10.1109/tcsi.2010.2071730